Supplemental Material:

Unraveling the lattice thermal conductivity and thermoelectric properties of monolayer Mg_3Bi_2

Yingying Chen[a], Zheng Ma[b,c], Na Zhao[d], Yajun Li[e], Xi Yao[f], Xilong Dou[f] *

[a] *College of Physics and Electronic Information Engineering*, *Hubei Engineering University*, *Xiaogan*, *Hubei 432000*, *China*

[b] *School of Automobile, Chang'an University, Xi'an, Shaanxi* 710064*, China*

[c] *Department of Mechanical Engineering, Texas A&M University, College Station*, *TX 77840 USA*

[d] *School of Finance and Economics Management, Sichuan University of Arts and Science, Dazhou, Sichuan 635000, China*

[e] *Engineering Research Center of Integrated Circuit Packaging and Testing, Ministry of Education, Tianshui Normal University, Tianshui, Gansu 741001, China*

[f] *School of Mathematics and Physics, Lanzhou Jiaotong University, Lanzhou, Gansu 730070, China*

* Corresponding author Email addresses: xilongdou369@163.com

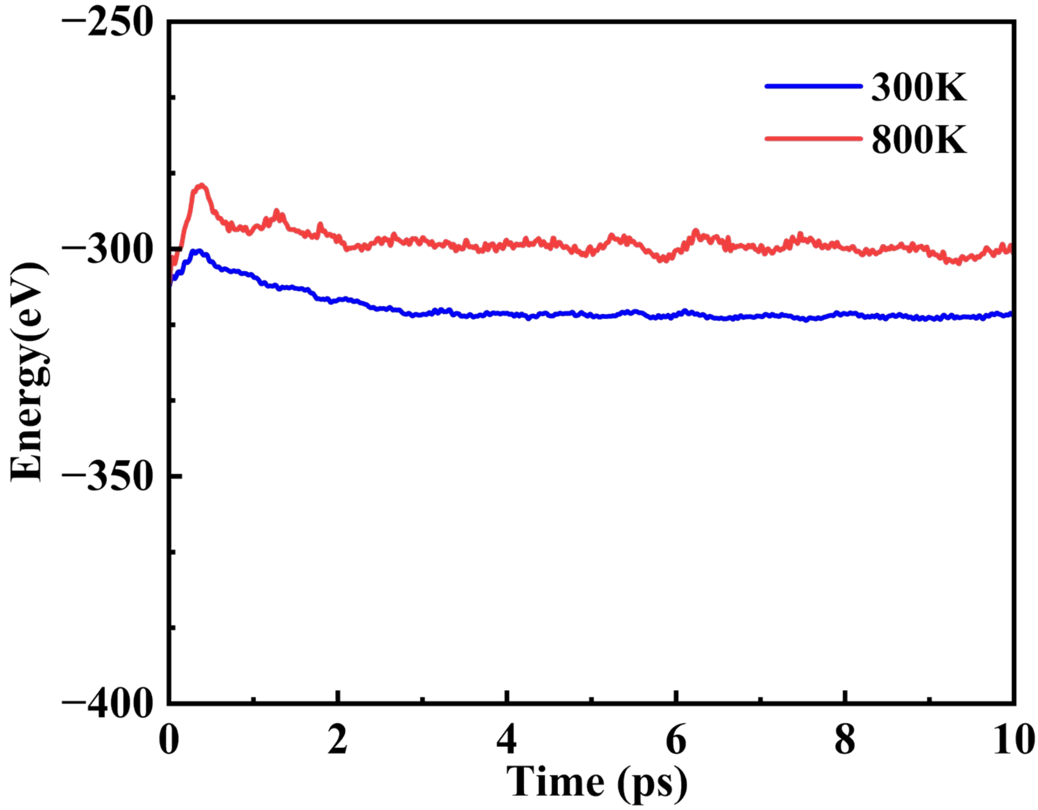

Fig. S1. Energy fluctuations of monolayer Mg_3Bi_2 in AIMD simulations at 300K and 800K.

The formation energy (E_f) of each structure can be calculated by the following formula:

$$E_f = (E_{total} - n_{Mg}E_{Mg} - n_{Bi}E_{Bi})/(n_{Mg} + n_{Bi}) \quad (1)$$

where E_{total}, E_{Mg} and E_{Bi} are the total energy of the system, the energy of Mg and Bi atoms, respectively. n_{Mg} and n_{Bi} are the number of Mg and Bi atoms in the unit cell, respectively.

The elastic energy $U(\varepsilon)$ of 2D materials using standard Voigt notation can be expressed as [1]:

$$U(\varepsilon) = \frac{1}{2}C_{11}\varepsilon_{xx}^2 + \frac{1}{2}C_{22}\varepsilon_{yy}^2 + C_{12}\varepsilon_{xx}\varepsilon_{yy} + 2C_{66}\varepsilon_{xy}^2, \quad (2)$$

where the ε_{ij} (i,j=x,y) and C_{ij} (i,j=1, 2, 6) are the strain tensors and elastic constants, respectively. The C_{ij} can be gained from the second partial derivative of strain energy with respect to strain ($C_{ij} = (1/S_0)(\partial^2 U(\varepsilon)/\partial\varepsilon_i\partial\varepsilon_j)$, where S_0 is the area of the equilibrium unit cell. The strain range is from -2% to 2% with the step of 0.05%. Meanwhile, the orientation-dependent mechanical properties, including the in-plane Young's modulus $E(\theta)$ and Poisson's ratio $\nu(\theta)$, can be calculated based on the elastic constants via the following equations [2]:

$$E(\theta) = \frac{C_{11}C_{22} - C_{12}^2}{C_{11}sin^4\theta + C_{22}cos^4\theta + (\frac{C_{11}C_{22} - C_{12}^2}{C_{66}} - 2C_{12})sin^2\theta cos^2\theta} \quad (3)$$

$$v(\theta) = \frac{C_{12}(sin^4\theta + cos^4\theta) - \left(C_{11} + C_{22} - \frac{C_{11}C_{22} - C_{12}^2}{C_{66}}\right)sin^2\theta cos^2\theta}{C_{11}sin^4\theta + C_{22}cos^4\theta + \left(\frac{C_{11}C_{22} - C_{12}^2}{C_{66}} - 2C_{12}\right)sin^2\theta cos^2\theta} \quad (4)$$

The orientation-dependent *Y(θ)* and *υ(θ)* and the corresponding polar diagram are plotted in Fig. S1. The Voigt and Reuss estimated bulk (B^V,B^R) and shear moduli (G^V, G^R) of 2D materials can be calculated from the following formulas [3, 4]:

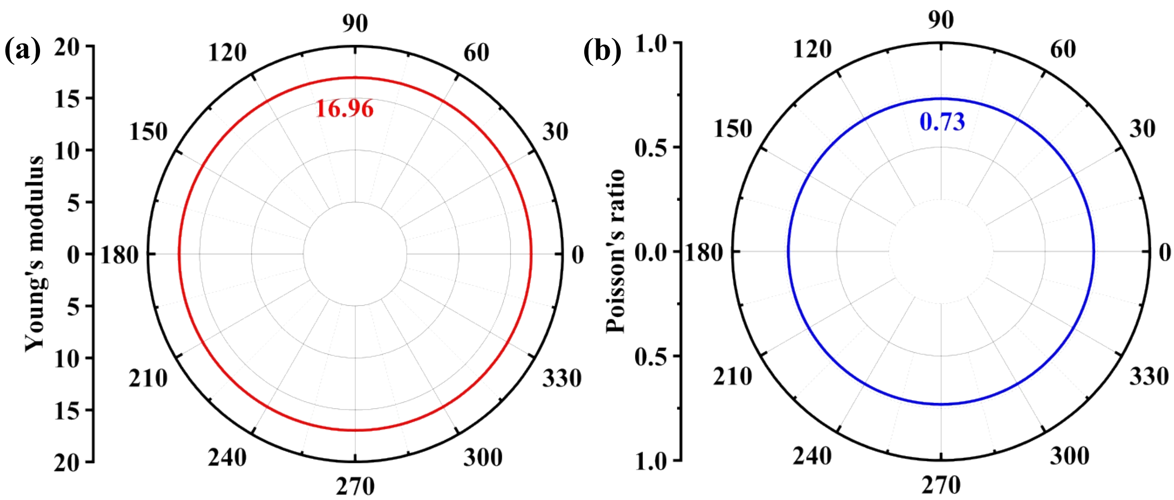

$$B^V = B^R = \frac{C_{11} + C_{12}}{2}, \quad (5)$$

$$G^V = G^R = \frac{C_{11} - C_{12}}{2}, \quad (6)$$

$$B = (B^V + B^R)/2, \quad (7)$$

$$G = (G^V + G^R)/2, \quad (8)$$

where *B* and *G* represent bulk (*B*) and shear modulus, respectively. The calculated results are shown in Table S1.

Fig. S2. Orientation-dependent (a) Young's modulus and (b) Poisson's ration for monolayer Mg_3Bi_2.

Table S1. Elastic constants, elastic compliance constants, bulk modulus, shear modulus, Young's modulus, and Poisson's ratio for monolayer Mg_3Bi_2.

Structure	C_{11}=C_{22} (N/m)	C_{12} (N/m)	C_{66} (N/m)	S_{11} (m/N)	S_{12} (m/N)	S_{66} (m/N)	*B* (N/m)	*G* (N/m)	*v*	*E* (N/m)
Mg_3Bi_2	36.49	26.69	4.90	0.058	-0.043	0.204	31.59	4.89	0.73	16.96

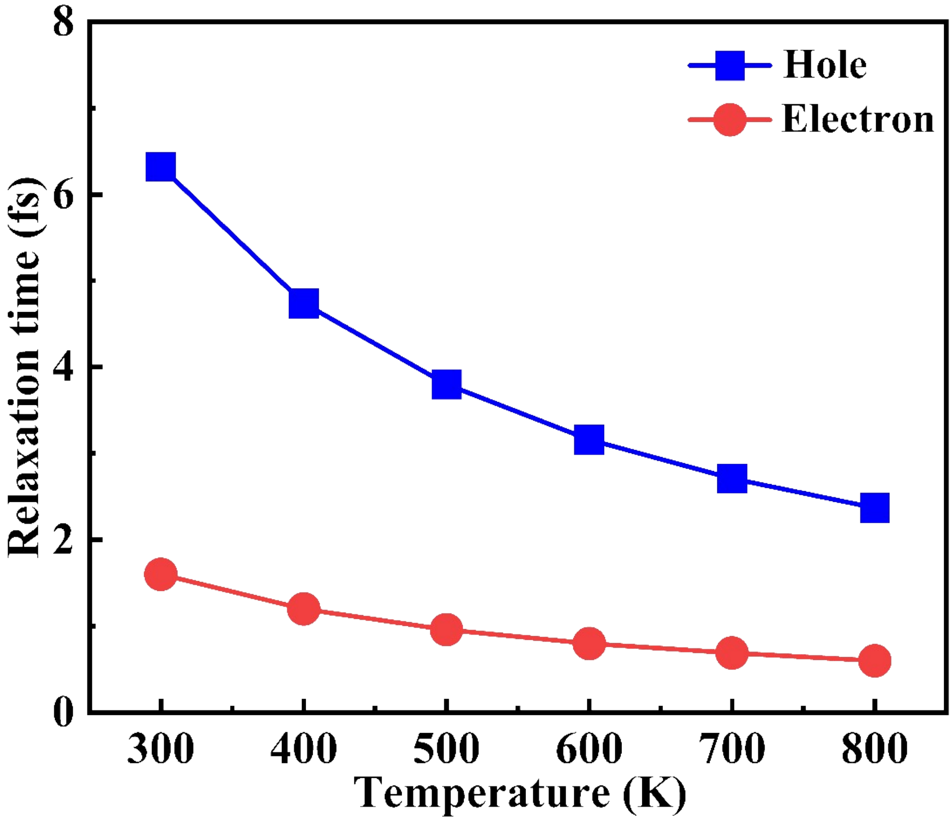

Fig. S3. Relaxation time for monolayer Mg_3Bi_2.

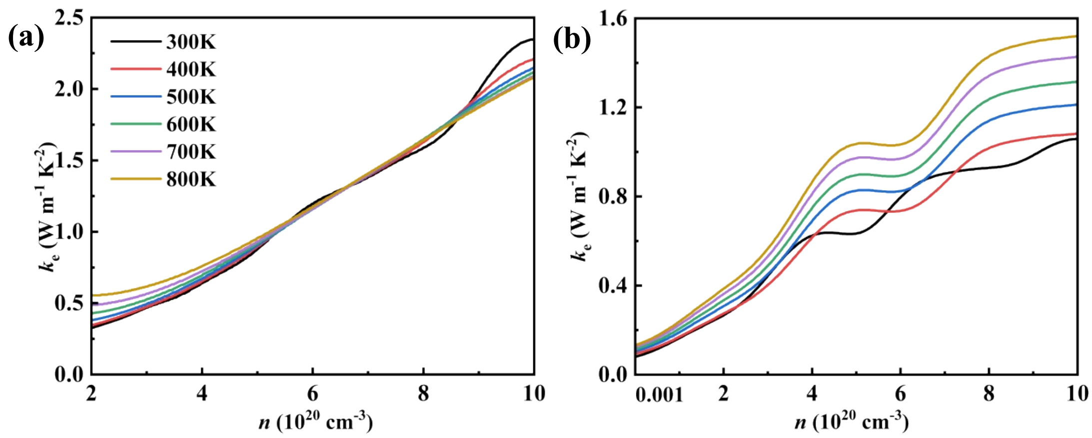

Fig. S4. Electrical thermal conductivity k_e as a function of carrier concentration for (a) *p*-type and (b) *n*-type monolayer Mg_3Bi_2.

Table S2. Comparison of electrical properties of *p*-type monolayer Mg_3Bi_2.

Methods	n (10^{20} cm^{-3})	σ (10^4 S m^{-1})	S (μVK^{-1})	PF (mWm^{-1}K^{-2})	ZT	T (K)	Refs.
DFT	5.07	12.26	50.60	0.32	0.08	300	This work
Magnetron sputtering	4.24	17.20	45.76	0.32	0.08	300	[5]
Magnetron sputtering	/	39.46	52.8	1.1	/	393	[6]
Magnetron sputtering	4	29.41	82	1.97	/	300	[7]
Magnetron sputtering	/	32.05	53	0.89	/	565	[8]
Thermal evaporation	4.5	83.5	60.1	3.02	0.11	473	[9]

References

[1] B. Peng, H. Zhang, H. Shao, Y. Xu, G. Ni, and R. Zhang, Phonon transport properties of two-dimensional group-IV materials from ab initio calculations, Phys. Rev. B 94, (2016): 245420.

[2] Y. Xu, Y. Liu, Y. Chen, Y. Zhang, C. Ma, H. Zhang, S. Sun, and Y. Ji, ACS Appl. Mater. Interfaces 12, (2020): 58349-58359.

[3] R. Li, Q. Shao, E. Gao, and Z. Liu, Elastic anisotropy measure for two-dimensional

crystals, Extreme Mech. Lett. 34, (2020): 100615.

[4] Z. Wu, E. Zhao, H. Xiang, X. Hao, X. Liu, and J. Meng, Crystal structures and elastic properties of superhard IrN_2 and IrN_3 from first principles, Phys. Rev. B 76, (2007): 054115.

[5] Y. Ran, W. Ma, H. Yu, W. Li, D. Zhou, F. Wang, N. Gao, Z. Yu, and K. Tai, Enhanced thermoelectric performance of $Mg_3Sb_{2-x}Bi_x$ thermoelectric thin films through carrier concentration modulation by Bi alloying, J. Alloys Compd. 985, (2024): 174028.

[6] W. Fang, W. Zhu, Y. Shao, P. Zheng, J. Si, Formation of metastable cubic phase and thermoelectric properties in Mg3Bi2 films deposited by magnetron sputtering, Appl. Surf. Sci. 596, (2022) 153602.

[7] G. Sadowski, Y. Zhu, R. Shu, T. Feng, A. Febvrier, D. Music, W. Liu, P. Eklund, Epitaxial growth and thermoelectric properties of Mg_3Bi_2 thin films deposited by magnetron sputtering, Appl. Phys. Lett. 120, (2022) 051901.

[8] J. Tani, H. Ishikawa, Fabrication and analysis of Mg_3Bi_2 thin films by post annealing Mg/Bi bilayer thin films, Mater. Lett. 331, (2022) 133460.

[9] J. W. C. Reinders, C. Roldán-Carmona, H.J. Bolink, F. Palazon, Tunable p- and n-Type Tellurium-Free Mg_3Bi_2 Thermoelectric Thin Films by Thermal Coevaporation, ACS Appl. Energy Mater. 6, (2023) 10327-10332.